

Performance analysis of GaN-based high-electron-mobility transistors with postpassivation plasma treatment

Xing-Ye Zhou(周幸叶), Xin Tan(谭鑫), Yuan-Jie Lv(吕元杰), Guo-Dong Gu(顾国栋), Zhi-Rong Zhang(张志荣), Yan-Min Guo(郭艳敏), Zhi-Hong Feng(冯志红), and Shu-Jun Cai(蔡树军)

Citation: Chin. Phys. B, 2021, 30 (**2**): 028502. DOI: 10.1088/1674-1056/abb7f6
Journal homepage: http://cpb.iphy.ac.cn; http://iopscience.iop.org/cpb

What follows is a list of articles you may be interested in

In-memory computing to break the memory wall

Xiaohe Huang(黄晓合), Chunsen Liu(刘春森), Yu-Gang Jiang(姜育刚), Peng Zhou(周鹏)
Chin. Phys. B, 2020, 29 (**7**): 078504. DOI: 10.1088/1674-1056/ab90e7

Photoresponsive characteristics of thin film transistors with perovskite quantum dots embedded amorphous InGaZnO channels

Mei-Na Zhang(张美娜), Yan Shao(邵龑), Xiao-Lin Wang(王晓琳), Xiaohan Wu(吴小晗), Wen-Jun Liu(刘文军), Shi-Jin Ding(丁士进)
Chin. Phys. B, 2020, 29 (**7**): 078503. DOI: 10.1088/1674-1056/ab9738

High-performance inverters based on ambipolar organic-inorganic heterojunction thin-film transistors

Sheng Sun(孙圣), Yuzhi Li(李育智), Shengdong Zhang(张盛东)
Chin. Phys. B, 2020, 29 (**5**): 058503. DOI: 10.1088/1674-1056/ab7e96

Stackable luminescent device integrating blue light emitting diode with red organic light emitting diode

Kang Su(苏康), Jing Li(李璟), Chang Ge(葛畅), Xing-Dong Lu(陆兴东), Zhi-Cong Li(李志聪), Guo-Hong Wang(王国宏), Jin-Min Li(李晋闽)
Chin. Phys. B, 2020, 29 (**4**): 048504. DOI: 10.1088/1674-1056/ab77ff

Experimental and computational study of visible light-induced photocatalytic ability of nitrogen ions-implanted TiO_2 nanotubes

Ruijing Zhang(张瑞菁), Xiaoli Liu(刘晓丽), Xinggang Hou(侯兴刚), Bin Liao(廖斌)
Chin. Phys. B, 2020, 29 (**4**): 048501. DOI: 10.1088/1674-1056/ab6d53

Performance analysis of GaN-based high-electron-mobility transistors with postpassivation plasma treatment*

Xing-Ye Zhou(周幸叶), Xin Tan(谭鑫), Yuan-Jie Lv(吕元杰)†, Guo-Dong Gu(顾国栋), Zhi-Rong Zhang(张志荣), Yan-Min Guo(郭艳敏), Zhi-Hong Feng(冯志红)‡, and Shu-Jun Cai(蔡树军)§

National Key Laboratory of Application Specific Integrated Circuit, Hebei Semiconductor Research Institute, Shijiazhuang 050051, *China*

(Received 16 July 2020; revised manuscript received 28 August 2020; accepted manuscript online 14 September 2020)

AlGaN/GaN high-electron-mobility transistors (HEMTs) with postpassivation plasma treatment are demonstrated and investigated for the first time. The results show that postpassivation plasma treatment can reduce the gate leakage and enhance the drain current. Comparing with the conventional devices, the gate leakage of AlGaN/GaN HEMTs with postpassivation plasma decreases greatly while the drain current increases. Capacitance–voltage measurement and frequency-dependent conductance method are used to study the surface and interface traps. The mechanism analysis indicates that the surface traps in the access region can be reduced by postpassivation plasma treatment and thus suppress the effect of virtual gate, which can explain the improvement of DC characteristics of devices. Moreover, the density and time constant of interface traps under the gate are extracted and analyzed.

Keywords: GaN, HEMT, gate leakage, trapping effect

PACS: 85.30.Tv, 85.30.De, 73.61.Ey, 73.50.Gr **DOI:** 10.1088/1674-1056/abb7f6

1. Introduction

Owing to the advantages of material properties, such as high electron mobility, high breakdown electric field, and high thermal conductivity, GaN-based high-electron-mobility transistors (HEMTs) have attracted lots of interest and achieved excellent successes in the past few years.[1–4] However, further performance improvements of these devices are limited by high gate leakage and small gate swing.[5,6] The gate leakage in AlGaN/GaN HEMTs and InAlN/GaN HEMTs have been widely investigated.[7–16] For device fabrication, surface passivation is usually adopted, which can effectively suppress the *I*–*V* hysteresis and current collapse induced by trapping effect in the access region. Nevertheless, the gate leakage will probably increase after passivation,[17,18] which is unexpected.

In this paper, AlGaN/GaN HEMTs with postpassivation plasma treatment are investigated for the first time. Comparing with the conventional devices, the results demonstrate that the gate leakage is greatly reduced, while the drain current is increased for AlGaN/GaN HEMTs with postpassivation plasma treatment. In order to study the influence of postpassivation plasma treatment on the surface and interface traps, capacitance–voltage measurement and frequency-dependent conductance method are used. It is shown that the improvement of direct current (DC) characteristics of devices is due to minimizing the virtual gate effect, which can be attributed to the suppression of surface traps in the access region by postpassivation plasma treatment. Moreover, the density and time constant of interface traps under the gate are also extracted and analyzed.

2. Device structure and fabrication

The AlGaN/GaN epi-layer structure in this work was grown by metal–organic chemical vapor deposition (MOCVD) on SiC substrate, which was composed of a 2-μm-thick undoped GaN layer, a 1-nm-thick AlN inserting layer and a 26-nm-thick $Al_{0.2}Ga_{0.8}N$ barrier layer.

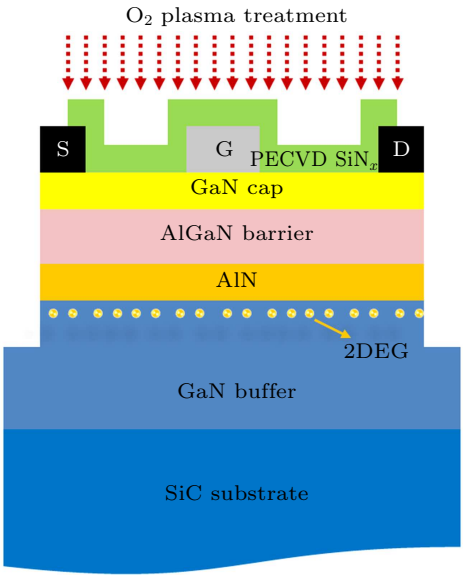


Fig. 1. Schematic cross-sectional structure of AlGaN/GaN HEMT.

*Project supported by the National Natural Science Foundation of China (Grant Nos. 61674130 and 61804139).

†Corresponding author. E-mail: yuanjielv@163.com

‡Corresponding author. E-mail: ga917vv@163.com

§Corresponding author. E-mail: ececai@126.com

© 2021 Chinese Physical Society and IOP Publishing Ltd

A two-dimensional electron gas (2DEG) with a density of 8.84×10^{12} cm^{-2} and an electron mobility of 2066 cm^2·V^{-1}·s^{-1} was obtained based on the room-temperature Hall measurement. For the device fabrication, the mesa isolation was formed first by inductively coupled plasma (ICP) dry etching. Source/drain electrode contacts with Ti/Al/Ni/Au metal stack formed, followed by rapid thermal annealing at 810 °C for 30 s in N_2 atmosphere. After that, the gate electrode with Ni/Au (50/200 nm) stack was deposited by electron-beam evaporation. For passivation, 100-nm-thick SiN_x layer was grown by plasma enhanced chemical vapor deposition (PECVD) with SiH_4/NH_3 (200/3 sccm) under an RF power of 20 W at 250 °C. Then, the SiN_x layer in the electrode contact region was opened by ICP etching. After removing the photoresist, the O_2 plasma treatment on the wafer was finally carried out with an RF power of 50 W for 3 min in a plasma treatment system. In order to investigate the traps by using capacitance–voltage measurement and frequency-dependent conductance method, an FAT device was fabricated in this work. The gate length and width were $L_g = 20$ μm and $W = 100$ μm, respectively. The gate–source spacing was 10 μm with a drain–source distance of 100 μm. The schematic cross section structure of AlGaN/GaN HEMT is shown in Fig. 1.

3. Results and discussion

First, the direct current (DC) characteristics of the fabricated AlGaN/GaN HEMT are measured as plotted in Fig. 2. Figures 2(a)–2(c) show the comparison of gate leakage, transfer and output characteristics between devices with and without postpassivation plasma treatment, respectively. As seen from Fig. 2, the gate leakage is reduced by almost 3 orders of magnitude compared with that of the device without postpassivation plasma treatment. In addition, the drain current increases after the devices have been plasma-treated. The performance improvement may be due to the suppression of trap-induced virtual gate effect, which will be discussed in detail below.

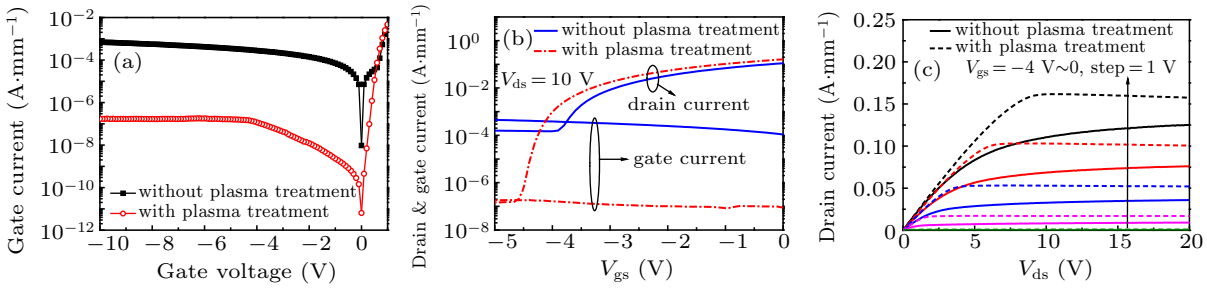


Fig. 2. Comparison of DC characteristics between AlGaN/GaN HEMT with and without plasma treatment, showing (a) gate leakage, (b) transfer characteristics, and (c) output characteristics.

Capacitance–voltage measurements with different frequencies are carried out, the results are shown in Fig. 3, where the *C*–*V* curves are obtained by using gate and source contact. It can be seen from Fig. 3(a) that there exists frequency-dependent capacitance dispersion in HEMT without plasma treatment, indicating a trapping effect. With the postpassivation plasma treatment, the capacitance dispersion is negligible [see Fig. 3(b)]. As is well known, the traps at the 2DEG interface can cause the threshold voltage to shift. However, there is observed no threshold voltage V_{th} dispersion in devices with or without plasma treatment. This means that the capacitance dispersion at zero or low reverse voltage for devices without plasma treatment may be induced by the traps in the access region. The postpassivation plasma treatment can reduce the surface traps in the access region, consequently leading the capacitance dispersion to be suppressed. Moreover, the decrease of gate leakage current in Fig. 2 can also be attributed to the reduction of surface traps, where the surface leakage path is blocked due to the postpassivatioin plasma treatment. The postpassivation plasma treatment in this work may change the composition of SiN_x passivation layer. For example, the dangling bonds may be reduced or the nitrogen vacancies may be filled with oxygen atoms, thereby reducing the surface traps and blocking the leakage path in the access region.

Based on the *C*–*V* measurement results in Fig. 3, the 2DEG density under the gate of AlGaN/GaN HEMT can be calculated by following the algorithm in Ref. [19]. Figure 4 shows the calculated values of 2DEG density in AlGaN/GaN HEMT with and without the postpassivation plasma treatment. We can see that the 2DEG density increases after postpassivation plasma treatment. This can be explained by the traps-induced virtual gate effect. For the AlGaN/GaN HEMTs without the postpassivation plasma treatment, there are more surface traps in the access region, which can act as a virtual gate. The virtual gate will result in the reduction of 2DEG density, since the 2DEG density is dependent on the Schottky gate area.[19,20] With the postpassivation plasma treatment, the surface traps are effectively suppressed and thus the virtual gate effect is minimized. Consequently, the 2DEG density increases, which is consistent with the increase of drain current (see Fig. 2).

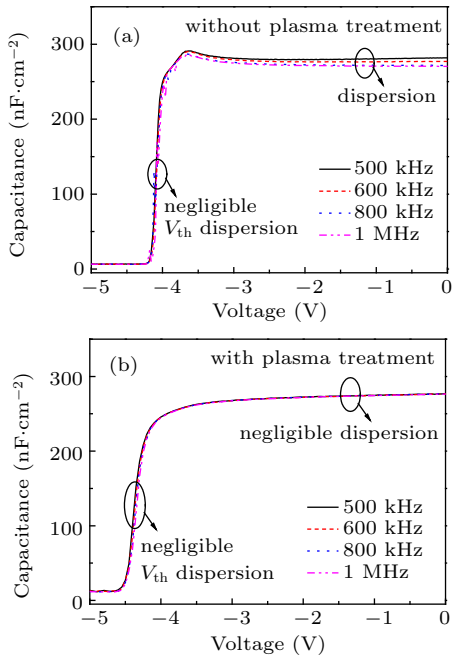


Fig. 3. Capacitance–voltage measurement results of AlGaN/GaN HEMT (a) without and (b) with postpassivatioin plasma treatment.

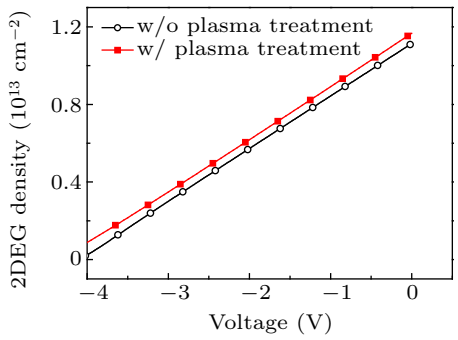


Fig. 4. Density of 2DEG *versus* voltage, obtained from *C*–*V* measurement for AlGaN/GaN HEMT with and without plasma treatment.

Finally, the interface trap density under the gate is extracted by the frequency-dependent conductance method. The small-signal equivalent circuits for frequency-dependent conductance measurement are shown in Fig. 5. The resistance R_{it} and capacitance C_{it} in Fig. 5(a) represent the interface traps with a time constant $\tau_{it} = R_{it} \cdot C_{it}$. Figure 5(b) shows the simplified circuit with a parallel capacitance C_p and conductance G_p. Under the assumption of continuous trap levels, the conductance G_p can be expressed as[21,22]

$$\frac{G_p}{\omega} = \frac{qD_{it}}{2\omega\tau_{it}} \ln\left[1 + (\omega\tau_{it})^2\right], \tag{1}$$

where $\omega = 2\pi f$ is the radial frequency, D_{it} is the trap density, and τ_{it} is the trap time constant.

Figure 6(a) shows the measurement results of frequency-dependent conductance G_p as a function of ω under different gate bias voltages for the AlGaN/GaN HEMT with the postpassivation plasma treatment, where the fitting results from Eq. (1) are also plotted. It can be seen that the model fitting results match the experimental data very well. The extracted interface trap density mapping is given in Fig. 6(b), and the interface traps exhibit short time constant. Therefore, the threshold voltage will not be affected by the fast interface traps, leading to the negligible frequency-dependent V_{th} shift in Fig. 3.

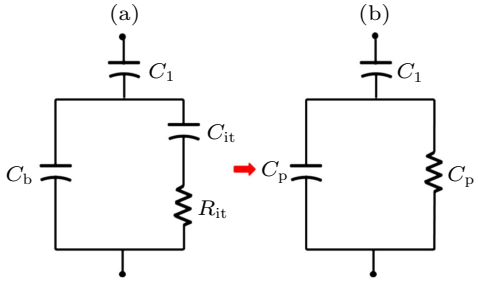


Fig. 5. Small-signal equivalent circuits for frequency-dependent conductance measurement, showing (a) gate capacitor with interface traps, and (b) simplified circuit used in conductance-based D_{it} analysis.

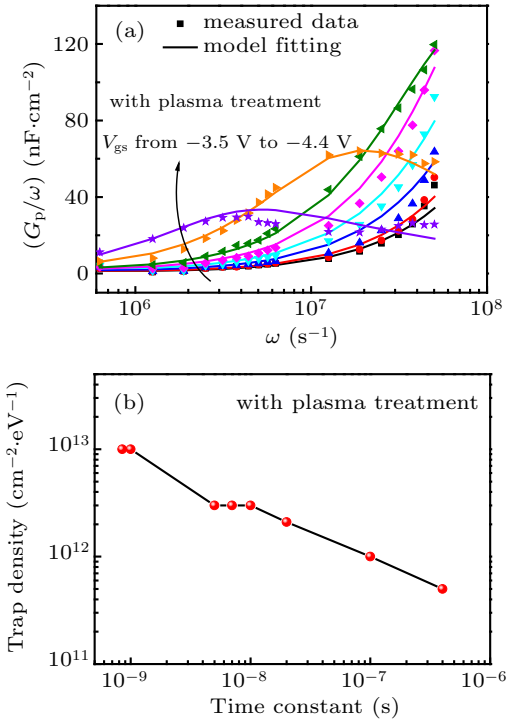


Fig. 6. Frequency-dependent conductance measurements of AlGaN/GaN HEMTs with postpassivation plasma treatment: (a) conductance as a function of radial frequency and (b) extracted trap density as a function of time constant.

4. Conclusions

In this work, AlGaN/GaN HEMTs with postpassivation plasma treatment are fabricated and investigated. It is demonstrated that comparing with the conventional devices, the gate leakage is effectively reduced, while the drain current is increased for AlGaN/GaN HEMTs with postpassivation plasma treatment. The surface and interface traps are studied based on the capacitance–voltage measurement and frequency-dependent conductance method. The improvement of DC characteristics of devices can be attributed to the suppression of virtual gate effect by the postpassivation plasma treatment. The results in this work can provide a reference for improving the performances of AlGaN/GaN HEMTs.

References

[1] Wu Y F, Saxler A, Moore M, *et al.* 2004 *IEEE Electron Dev. Lett.* **25** 117
[2] Hao Y, Yang L, Ma X H, *et al.* 2011 *IEEE Electron Dev. Lett.* **32** 626
[3] Pengelly R S, Wood S M, Milligan J W, *et al.* 2012 *IEEE Trans. Microw. Theory Tech.* **60** 1764
[4] Marti D, Tirelli S, Alt A R, *et al.* 2012 *IEEE Electron Dev. Lett.* **33** 1372
[5] Sanabria C, Chakraborty A, Xu H T, *et al.* 2006 *IEEE Electron Dev. Lett.* **27** 19
[6] Chung J W, Roberts J C, Piner E L, *et al.* 2008 *IEEE Electron Dev. Lett.* **29** 1196
[7] Xia L, Hanson A, Boles T, *et al.* 2013 *Appl. Phys. Lett.* **102** 113510
[8] Arslan E, Bütün S and Ozbay E 2009 *Appl. Phys. Lett.* **94** 142106
[9] Yan D, Lu H, Cao D, *et al.* 2010 *Appl. Phys. Lett.* **97** 153503
[10] Liu Z H, Ng G I, Arulkumaran S, *et al.* 2011 *Appl. Phys. Lett.* **98** 163501
[11] Hanna M J, Zhao H, and Lee J C 2012 *Appl. Phys. Lett.* **101** 153504
[12] Turuvekere S, Karumuri N, Rahman A A, *et al.* 2013 *IEEE Trans. Electron Dev.* **60** 3157
[13] Zhu J J, Ma X H, Hou B, *et al.* 2014 *Appl. Phys. Lett.* **104** 153510
[14] Dutta G, DasGupta N and DasGupta A 2017 *IEEE Trans. Electron Dev.* **64** 3609
[15] Sun Z H, Huang H L, Wang R H, *et al.* 2020 *IEEE Electron Dev. Lett.* **41** 135
[16] Cui X, Cheng W J, Hua Q L, *et al.* 2020 *Nano Energy* **68** 104361
[17] Bai L, Yan W, Li Z F, *et al.* 2016 *Chin. Phys. Lett.* **33** 067201
[18] Zhou X, Wang Y, Tan X, *et al.* 2019 *IEEE International Conference on Electron Devices and Solid-State Circuits,* June 12–14, 2019, Xi'an, China
[19] Zhao Z J, Lin Z J, Corrigan T D, *et al.* 2007 *Appl. Phys. Lett.* **91** 173507
[20] Lv Y J, Feng Z H, Gu G D, *et al.* 2015 *Chin. Phys. B* **24** 087306
[21] Zhu J J, Ma X H, Xie Y, *et al.* 2015 *IEEE Trans. Electron Dev.* **62** 512
[22] Lu X, Yu K, Jiang H, *et al.* 2017 *IEEE Trans. Electron Dev.* **64** 824